TRACKING DETECTORS FOR LARGE HADRON COLLIDERS AND FOR e^+e^- LINEAR COLLIDERS

E. Elsen and A. Wagner

Physikalisches Institut, Universität Heidelberg, Fed. Rep. Germany

Abstract

First , a design concept for a central tracking chamber for use at a large hadron collider is presented. Its characteristic features are a built-in rejection of out -of-time tracks by means of a jet cell geometry and multihit read-out electronics. The design is optimized to provide local recognition of genuine trigger tracks and local rejection of out-of-time hits. In a simple simulation of the cell configuration it can be shown, that the large occupancy resulting from the long drift paths does neither lead to a significant fraction of fake tracks nor to a big loss of genuine tracks. In addition, a study is presented of a tracking detector for an e^+e^- collider with the main emphasis on the questions how well systematic contributions to the momentum error can be controlled.

1. Introduction

The study group on vertex detection and tracking at a future European accelerator has reviewed the relative merits of a large hadron collider (LHC) and of an e^+e^- linear collider (CLIC) with the main emphasis on the feasibility of tracking at both machines [1]. The present paper is an extension of work done for the study group. The biggest fraction of this paper is devoted to a specific proposal for a tracking chamber at LHC including a crude simulation of the detector response to jets and minimum bias background events. Since a tracking chamber at CLIC does not seem to pose any major problems, only the limits of the momentum resolution for tracks in the TeV range are analysed.

2. Basic Design Concept for a Tracking Detector at LHC

2.1 Outline of the Approach

While various reasons can be given showing the need for tracking at a large hadron collider, it is not at all clear if and by which technique one will be able to cope with the total number of tracks, the local particle density, and the radiation exposure expected at a machine with an interbunch distance of 15-25 ns, a luminosity of 10^{33} $cm^{-2}s^{-1}$ and a large total cross section of 100 mb. The most thorough design study of a possible central tracking detector was done at the 1986 Snowmass Summer Study [2]. There the central tracking group studied how to build a realistic central tracking system for a general purpose 4π detector for the SSC. The suggested solution for this tracking system was a small cell gas chamber using either wires or straw tubes. The group also considered tracking by scintillating fibres or silicon micro strips but came to the conclusion that neither of both is a realistic candidate given the current state of technology.

It has been shown that the biggest problem for tracking in a hadron collider with short interbunch distance is not the radiation damage, but the number of hits present in the chamber at any given time (occupancy). Some of these hits belong to the event which has caused the trigger, some belong to a minimum bias event from the same bunch crossing and many hits are due to tracks from earlier or later crossings.

The design presented at Snowmass was based on the requirement that the cell occupancy should be less than 10 %. As a consequence, when using standard drift chamber gases, one has to restrict the size of the drift cells to dimensions between 2 mm at a radius of 50 cm and 5 mm at r = 200 cm. With 120 layers of sense wires, grouped into four modules, one has to deal with 134.000 sense wires and 411.000 field wires. Even the optimist who sees a clear path through the haze of big cross section reactions to the shining world of the underlying physics is fearfully shying away from such a detector.

Do alternatives exist which have a significantly smaller number of sense and field wires? This requires obviously bigger drift cells and possibly faster gases than those used in present detectors. An unavoidable consequence of bigger cells is the considerable increase in occupancy and the key question is if such occupancies do or do not deteriorate the tracking performance.

In the design presented here a larger occupancy can be tolerated since out-of-time tracks are rejected using information provided by the chamber itself. This technique was already discussed at the 1984 LHC workshop at Lausanne [3]. Of the two solutions studied there, the tilted cell geometry is preferred after closer studies, since it is better adapted to the operation of the chamber in a high magnetic field and since mirror tracks cause less disturbance of the events, because they do not point to the interaction region. Only tracking in the central region ($|\eta| < 1.5$) is considered. Online data handling and data compression are one of the guidelines for the design of this detector.

2.2 Mechanical Structure

A schematic drawing of the proposed LHC central drift chamber is shown in Fig. 1. The cross section through one quadrant of the chamber is shown in Fig. 1a) where the shaded areas represent the active regions, the superlayers, of the chamber . Superlayers 1 - 3 cover a rapidity region of $|\eta| < 1.5$, whereas the last superlayer provides a restricted coverage up to $|\eta| < 1.2$. This is due to the fact that for reasons of electrostatic stability the total wire length is limited to 4 meters. The superlayer structure has the advantage that the chamber can be built in a modular way, but the uncertainty in the relative alignment of the modules can easily add a significant contribution to the overall momentum error.

Fig. 1 b) shows the the details of the cell and wire arrangement in the outermost superlayer. The cell design is of the jet chamber type, but the sense wire planes are rotated with respect to the radius vector by 45 degrees in each superlayer. Such a structure has several advantages:

For a given magnetic field (1 - 2 T) the resulting Lorentz angle of the drifting electrons can partly be compensated through the appropriate choice of the electric field configuration such, that the drift trajectories are on average orthogonal to the ionizing tracks. The inclined cell structure is therefore well adapted to a chamber operation in large magnetic fields.

The reconstruction of space coordinates from the measured drift times requires the knowledge on which side of the wire plane the track has passed. This left / right ambiguity can in principle be resolved through a staggered sense wire structure or through an inclined sense wire plane. In the second case the "mirror tracks" do not point to the center of the detector and can therefore easily be identified. Furthermore, since the mirror tracks are strongly inclined with respect to the true tracks they can not hide completely a true track due to the finite double track resolution.

The third and most important reason for an inclined wire plane is the fact that this geometry provides an excellent identification and rejection of out-of-time tracks. This can be seen in Fig. 2 where a track with its hits is superimposed on one cell. Also shown are the hits that would be seen if the track had passed through the chamber at the same location, but were out of time, i.e. originating from an earlier (-1) and later (+3) bunchcrossing, assuming a time distance between bunches of 25 ns. Wherever the tracks cross a cell boundary (sense wire plane or cathode), a discontinuity in the reconstructed track occurs for all out-of-time tracks. The prerequisite for the correct identification of intime tracks is, that the trigger uniquely identifies the bunch crossing responsible for the event.

2.3 Chamber Parameters

In table 1 the basic parameters of the drift chamber and the relevant machine parameters are summarized. The chamber is subdivided in radial direction into 6 modules, each containing one superlayer with 8 sense wires per superlayer, adding up to a total of 48 layers. The width of the jet cells is chosen such, that the rate of hits/wire/sec and therefore the "intime" occupancy is the same for all wires. As a consequense, the memory time and total occupancy increase linearly with radius. It will be shown below, that this increase in occupancy from 16 % at r = 50 cm to 34 % at r = 150cm, inside the rapidity interval covered by the chamber, does not pose any significant problem for the event reconstruction efficiency.

A second point of concern for the operation of a drift chamber in a high rate environment is radiation damage. It can be seen from table 1, that the accumulated charge per year does not exceed 0.1 C/cm/year, a value which is one order of magnitude below the "critical" limit [4]. Table 1 contains also the total number of sense and field wires. With 15000 sense wires and 49000 field wires, equally distributed over 6 modules, the chamber represents only a modest extrapolation in terms of wire numbers and electronic channels from existing systems. Even an increase is the number of layers by a factor of 2 to provide a total of 96 points/track would require only 30 000 sense wires.

2.4 Gas

The drift velocities of typical drift chamber gases lie all in the range of v_D = 50 μm/ns. The detector occupancy is directly proportional to the memory time and therefore inversely proportional to the drift velocity. It seems advantagous therefore to use a gas with a drift velocity considerably higher than 50 μm/ns. One possibility is CF_4 - A (20 : 80) with v_D = 120 μm/ns, which has already been tested in high rate MWPCs [5]. Measurements on space resolution in drift chambers operated with this gas do not exist, but the diffusion coefficient in pure CF_4 has been measured and found to be low, close to the thermal limit even for electric field of 0.25 kV/cm [6]. In the present study we assume that a gas with similar properties will be used, but clearly considerably more R&D work needs to be done in the field of fast gases. It should be pointed out, that in fast gases one faces the potential problem of very large Lorentz angles. This problem can only partly be removed by applying high drift fields.

2.5 Read out Electronics

Due to the high particle density in the core of a jet the best possible two track resolution is required to obtain a good efficiency for track finding. In fact, as will be shown later, it is mainly the two track resolution which determines the pattern recognition efficiency. At present the best two track resolution is obtained by a fast waveform sampling of the drift chamber signals, using a 100 - 200 MHz FADC. A two track resolution of 2 mm has been achieved with v_D = 50 μm/ns. The resolution might be further improved by an appropriate pulse shaping of the chamber signals (tail cancellation). The digitized signals are stored in a (cyclic) buffer from where they can be retrieved in case of a valid trigger.

Considerable progress has recently been made in the on-line data anlysis of the chamber signals in front end micro processor farms [7]. The tasks dealt with there so far (conversion of the pulse shape into a drift time and signal charge) are at present extended to include local calibration and pattern recognition, for a similar read out system for the OPAL jet chamber. With pattern recognition done online also the local track vectors will be known online for each superlayer. This information not only provides a significant data reduction (from hit coordinates to four vectors), but in addition allows to introduce a soft momentum cut (p > 1 ... 10 GeV/c) online.

3. Study of the Detector Response with Simulated Events

3.1 Detector Layout

For the simulation of the detector response to true events and background we concentrate on the outermost superlayer at r=150 cm, which, due to its large drift distance, has the highest occupancy. We approximate the cell structure shown in Fig. 1b) by a rectangular geometry (see for example

Fig. 4). Each cell contains 8 sense wires, the wire plane is tilted by 45 ^{o} with respect to the radius vector, the distance between sense wires is chosen to be 8 mm within a superlayer. Two adjacent superlayers with a relative azimuthal displacement of one full drift distance (15 mm) are modelled. With this arrangement every track traversing the superlayer crosses at least one cell boundary, the prerequisite for the local recognition of out-of-time tracks. In total, 7 cells in two adjacent superlayers are simulated in the program. This corresponds to a window of 50.4 mm in azimuthal width. Tracks are generated in this area which represents 0.5 % of the circumference at a radius of 150 cm (aspect ratio).

3.2 Event Generation and Event Structure

We have simulated two classes of events:
i) "minimum bias" events with 6 particles per rapidity interval and a mean event rate of 1.6 interactions per bunch crossing, and ii) events with a topology which should represent the "core" of a jet. For each bunch crossing (at a time T_0) we generate a minimum bias event (event type i)), according to Poisson statistics, using the mean particle density and interaction rate as given above, and assuming a total rapidity coverage of the chamber of $\Delta\eta = 3$.

The small fraction of tracks which actually hit the acceptance window chosen in the program is then propagated through the wire setup and the drift times are stored in the hit buffers of the corresponding wires . The same procedure is repeated several times at consecutive bunch crossings to fill the hit buffer with background information. Events of type ii) are all generated at T_0=125 ns. Here a fixed number of tracks (0-10) is generated inside the acceptance window and the drift times are recorded in addition to the usual background event.

3.3 Detector Response

In a real detector the data from each wire are continously written into a buffer memory which, at any given time, contains information not only coming from the actual bunch crossing but also information of past events. Since the maximum drift time is long compared to the time between bunches, also information from bunch crossings which occur after the event of interest can be contained in the memory area that is analysed for each trigger. This is illustrated in Fig. 3. Therefore, in the present simulation background events are generated at all bunch crossings from T_0= 0 ns up to T_0 = 250 ns, while the "jet events" are always generated at T_0=125 ns. A real detector operating with waveform digitisation would record the full history of events in a similar manner.

3.4 Chamber Resolutions

Todays large drift chambers reach single hit resolutions of 100 μm and a two track resolution better than 2.5 mm with waveform sampling techniques. We hope that these resolutions can be obtained even when using a fast gas such as CF_4 (v_d=120 μm/ns). (This might necessitate the use of

higher sampling frequencies, e.g. 200 MHz in the electronics) . In the model we therefore smear the hit coordinates with a gaussian resolution of sigma 100 μm. If two hits overlap in the hit buffer within 2.5 mm/v_d = 21ns the later hit is discarded to account for the effects of the finite two track resolution.

3.5 Magnetic Field and Momentum Resolution

Over the small width of the superlayer the local curvature of most tracks can be neglected even in a 2.0 T field. At the radius of 150 cm, though, some tracks will have sufficiently large angles to deviate noticeably from perpendicular incidence. It is only in this respect that the effect of the magnetic field is taken into account. With a single hit resolution of 100 μm, a field of 2.0T and a track length of 110 cm the expected momentum resolution is 56 % at a momentum of 1 TeV/c.

3.6 Examples of Events

Fig. 4 shows an event with 5 tracks of the jet within the acceptance window. Even though there are 2 additional background tracks passing at other bunch crossings, but during the memory time, the in-time hits can be uniquely assigned. Mirror hits pose no problem at all. Out-of-time hits appear as a random background. This background only looks meaningful (such that one can recognize tracks) when analysed at the time of the corresponding bunch crossing (Fig. 5). All jet trigger tracks have dissolved into background hits whereas hits associated with the minimum bias event at T_0 = 175 ns can be clearly recognized. Two of the jet tracks in Fig. 4 come so close to each other that due to the finite two-track resolution they interfere with each other. Depending on the wire side, only one or the other track is seen. It will depend both on the homogenity of the chamber and the sophistication of the pattern recognition how many tracks actually are reconstructed. The impression from scanning a larger number of events is that the quantity limiting the pattern recognition efficiency is, in fact, the two track resolution. Background from out-of-time hits seems to be rather small. We try to quantify this a little further in the following.

3.7 Track Reconstruction

Since even at a radius of 150 cm most tracks are perpendicular to the effective drift direction, tracks are sufficiently well characterized by a single parameter: the coordinate x along the drift direction. A histogram of this coordinate for the hits in each layer develops a peak at the positions of true tracks, whereas mirror hits and out-of-time hits only contribute to a rather flat background in the histogram. The efficiency of such a method depends on the thresholds used in the peak search. Low thresholds increase the efficiency but also increase the fraction of fake tracks. To establish a track we require more than three entries in the bin of the peak (width=200 μm) after summation over 16 layers. We derive the azimuthal coordinate x of the track parameter from a bin weighted average of the entries around the peak.

We note several deficiencies of this "pattern recognition": Since no hits are individually assigned to tracks, no judgement is made on whether a hole (with no hits on the track) is reasonable. No check is performed on whether the hits contributing to the peak are actually compatible with the track within the given resolution. No checks are performed to see whether the background hits are actually compatible with a real track when the event is analyzed at different T_0 values. Due to all these effects the pattern recognition efficiency as evaluated below is probably underestimated. With the capabilities of investigating preceeding as well as following interactions many background hits can be unambiguously recognized and discarded. We apply this histogramming method nevertheless because it is fast to implement.

3.8 Reconstruction Efficiencies Using a Fast Gas

We calculate the reconstruction efficiencies by correlating the reconstructed tracks with the generated tracks. Tracks that cannot be associated with generated tracks are called fake tracks. Fig. 6 shows the efficiency for finding tracks as a function of the number of tracks in a jet. Even at 10 tracks/jet this number is still 70 %. Ten tracks in an acceptance of 50.4 mm at 150 cm radius would correspond to 0.03 tracks/mrad. This is close to the track density in the case of a jet, expected from a Monte Carlo simulation using existing event generators [8]. For five tracks the efficiency is above 80 %.

The fraction of fake tracks is quite independent of the number of generated tracks and is always well below 10 %. The values are probably better characterized as a fraction/event. Fig. 7 shows that for a jet event with five tracks into the acceptance only 0.5 additional tracks are reconstructed per event from confused hits of out-of time tracks.

3.9 Reconstruction Efficiencies Using a Standard Gas

For comparison the same simulation was repeated under the assumption that a "standard" drift chamber gas is used. The exact parameters taken for the calculations are v_D= 50 μm/ns, a two-track-resolution of 2 mm, and a point resolution of 100 μm. It should be noted that these performance values have already been reached in large drift chamber systems. The resulting efficiencies for finding true and fake tracks are also plotted in Fig. 6 and 7. One observes that, compared with a fast gas, for the standard gas the efficiency to reconstruct the true tracks is higher by 5-10%, mainly because of the better two-track resolution. On the other hand the probability to find fake tracks increases by a factor 2, due to the increase in memory time in case of the slower standard gas. Since all the efficiency numbers quoted here are evaluated on the basis of 2 superlayers only, the rejection of fake tracks might be improved when using the information from the entire detector.

Based on these numbers it is not excluded to use a standard gas, even in the case of large drift cells, especially if the two-track resolution could be improved further. Also the problem that in fast gases one has to cope with a large Lorentz angle becomes much easier in standard gases.

4. Tracking at an e^+e^--Collider in the TeV Range (CLIC)

The tracking environment which one faces at an e^+e^- collider in the TeV range is of a completely different nature. Since the total cross section is low and equal to the "interesting" cross section and since the time between collisions is 170 μs, neither occupancy, nor hit rate / wire, nor radiation damage pose any problems. (First estimates of beam strahlung indicate that the photon background from this source is essentially directed foreward and does not reach the tracking chamber). Therefore, present techniques can directly be applied for tracking at CLIC. For this study we did not attempt to produce a design for a tracking chamber, but considered only the question how far the momentum resolution could be pushed, particularly, if a value of $\Delta p / p = 10\%$ could be reached for tracks with a momentum of 1 TeV/c.

Assuming a measured tracklength of L = 2 m and a magnetic field of 2 T, the resulting sagitta of a track with p = 1 TeV/c is s = 300 μm. The requirement, that the momentum error should be 10% means that also the sagitta must be measured with an error of $\Delta s / s = 10\%$. Two sources contribute to this sagitta error: the measurements errors of the track coordinates and errors due to systematic track distortions. In order to estimate the sagitta error due to the measurement errors, we assume $\sigma_{R\phi} = 50$ μm per point, and N = 160 points on each track. This yields a ds/s = 5%, or ds = 15 μm. A point resolution of 50 μm seems feasible when using a slow, cool gas. Such a gas has two more advantages: it provides a good two-track resultion and the Lorentz angle of the drifting electrons is very small due to the slow drift velocity.

With a sagitta error of only 15 μm due to the measurement uncertainties it is obvious that the main limitation of the momentum resolution lies is the systematic errors. How well can those be controlled in a chamber of 4m diameter ? Tremendous progress has been made in the control of systematic errors through the use of UV-Lasers [9]. The straight tracks produced by the laser throughout the chamber volume allow not only a precise monitoring of the drift velocity, the Lorentz angle, time offsets etc., but help also to identify and correct for distortions of the wire supports, the electric fields, and the chamber body.

For a chamber which heavily relies on this laser calibration one would not chose a superlayer structure with small jet cells like in the LHC design, since there the many wires would block or deflect the laser beam, but one would probably take a wire plane structure with no radial subdivision as in the OPAL jet chamber, for two reasons: i) The laser beams can fully traverse the chamber in radial direction. ii) Most of the very high momentum tracks stay within the same radial segment of the chamber which leads to a first order cancellation of most systematic errors. First tests of the laser calibration in the OPAL jet chamber have shown [10], that using this technique the remaining systematic sagitta error is $ds \leq 30\mu m$ in a chamber of simular dimensions as the one discussed here. This result indicates that it should be possible to build a tracking detector for CLIC which provides a momentum resolution of about 10%.

5. Conclusion

5.1 Tracking at a Large Hadron C=ollider

Using a simple model the question is investigated in how much a large occupancy limits the track finding efficiency of a drift chamber of a jet cell type. The conclusion is, that despite high values of occupancy for each wire (around 35 %), out-of-time hits can be safely recognized in most cases. With the option of analyzing a given event with the assumption that it originates from different bunch crossings, the background from out-of-time hits can be made negligible. The true limitation comes from the finite two track separation. Even with 2.5 mm two track resolution the ability to find all tracks in the core of the jet is severely affected.

However, a geometry with small cells and single hit electronics would produce even higher inefficiencies. Comparatively large cells with multihit electronics operated in a fast gas seem to be the appropriate solution. Fortunately, the number of wires in such a setup will also be tolerable. The encouraging results presented here should be taken as stimulus to perform a more realistic simulation than the one developped for this study, and to pursue the question of the relative merits of fast and standard gases.

It must be pointed out that all present calculations are done assuming a time between bunches of 25 ns and an interaction rate/crossing of 1 - 2. With a total cross section of 100 mb this corresponds to a luminosity of $6.4 \cdot 10^{32}$. In order to reach a value of 10^{33} either the interbunch distance must be further decreased or the interaction rate per crossing must be increased. It is not clear at present, if under these conditions tracking in the conventional sense would still be possible.

5.2 Tracking at an $e^{\pm}e^{-}$ collider

Tracking at an electron positron collider poses no serious additional problem as compared to tracking at LEP or SLC. It is shown, that a momentum resulution of about 10% at 1 TeV can be reached by using a slow, cool gas and a laser calibration system of a similar sophistication as used in some of the present LEP detectors.

Acknowledgement

We would like to thank our cheerful group leader, Dr. David H. Saxon, for many stimulating discussions and for the pressure he put on us to produce a writeup of this work. One of us (E.E.) would like to thank the organisers of the 1986 Snowmass Study and APS for the support they provided during the Snowmass study week. This work has been funded in part by the German Federal Minister for Research and Technology (BMFT).

References

[1] D. M. Saxon, these proceedings
[2] D. G. Cassel and G. G. Hanson, SLAC-PUB-4130, to appear in Proc. 1986 Summer Study on the Physics of the Superconducting Super Collider, Snowmass, Colorado
[3] A. Wagner in Large Hadron Collider in the LEP Tunnel, ECFA 84/85, CERN 84-10, Vol. I, pp 267-281
[4] J. Vavra, Proc. Workshop on Radiation Damage to Wire Chambers (Ed J Kadyk, LBL-21170 (1986)) p 263
[5] J. Fischer, A. Hrisoho, V. Radeka and P. Rehak, Nucl. Instr. Meth. A 238, 249 (1985)
[6] B. Schmidt, Nucl.Instr. Meth. A 252, 579 (1986)
[7] G. Eckerlin et al., IEEE Trans. Nucl. Sci. NS 33, 1066 (1986)
[8] P.N. Burrows and G. Ingelman, these proceedings
[9] H. Hilke, Nucl. Instr. Meth. A 252, 169 (1986)
[10] H.M. Fischer et al., Nucl. Instr. Meth. A 252, 331 (1986)

Table I: Summary of Accelerator and Drift Chamber Parameters

time between bunches	ns	25.0						
Interactions / crossing		1.6						
Interactions / sec	MHz	64.00						
particles / rapidity interval		6						
drift velocity	micron/ns	120.00						
								Total
super layer number		**1**	**2**	**3**	**4**	**5**	**6**	
cells / layer		314	314	314	314	314	314	
sense wires / cell		8	8	8	8	8	8	48
field wires / cell		26	26	26	26	26	26	
sense wires / superlayer		2512	2512	2512	2512	2512	2512	15072
field wires / superlayer		8164	8164	8164	8164	8164	8164	48984
tracklength / layer	cm	0.8	0.8	0.8	0.8	0.8	0.8	
rmin	cm	50	70	90	110	130	150	
rmax	cm	55.60	75.60	95.60	115.60	135.60	155.60	
wire length	cm	220.00	310.00	400.00	400.00	400.00	400.00	
total rapidity coverage		3.06	3.06	3.06	2.72	2.44	2.20	
max drift distance	cm	0.50	0.70	0.90	1.10	1.30	1.50	
aspect ratio		0.0032	0.0032	0.0032	0.0032	0.0032	0.0032	
max drift time	ns	41.69	58.36	75.04	91.71	108.39	125.06	
memory time	bunch Xings	1.67	2.33	3.00	3.67	4.34	5.00	
< intime occupancy >		0.09	0.09	0.09	0.08	0.07	0.07	
< total occupancy >		0.16	0.22	0.28	0.31	0.32	0.34	
hits / wire/sec	MHz	3.74	3.74	3.74	3.33	2.98	2.69	
electrons / cm	1/cm	100	100	100	100	100	100	
gas gain		2.00E+04	2.00E+04	2.00E+04	2.00E+04	2.00E+04	2.00E+04	
current / wire	microAmp	0.96	0.96	0.96	0.85	0.76	0.69	
running time / year	sec	1.00E+07	1.00E+07	1.00E+07	1.00E+07	1.00E+07	1.00E+07	
accumulated charge	C/cm/year	0.044	0.031	0.024	0.021	0.019	0.017	

(the lines indicated with bold letters contain input parameters)

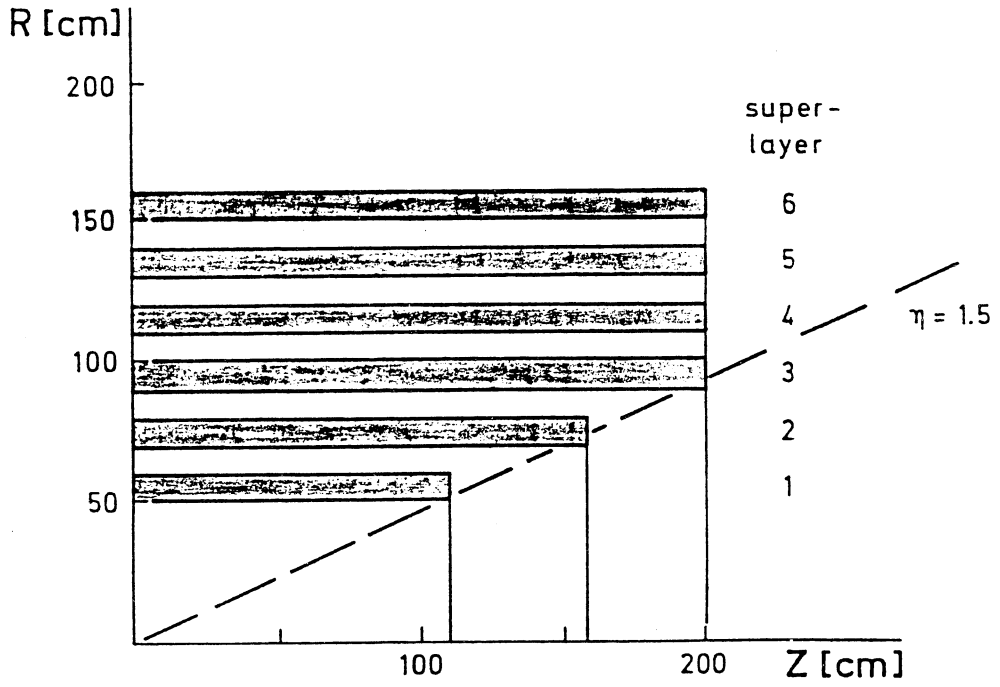

a) Schematic layout of the LHC Central Drift Chambers which is used as model

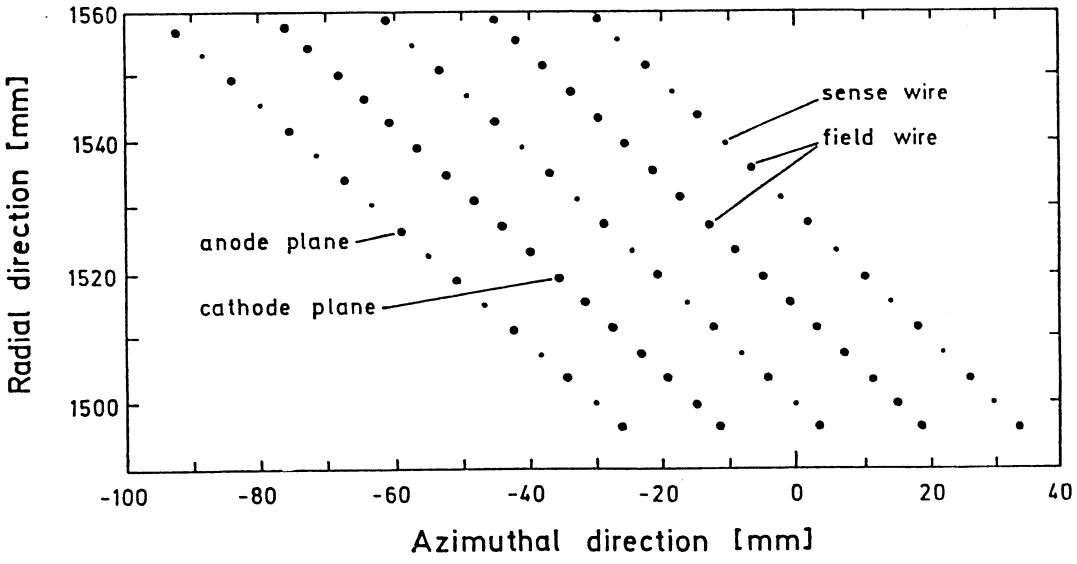

b) Detailed view of the wire arrangement and cell structure in superlayer 6 at r = 150 cm

Fig. 1

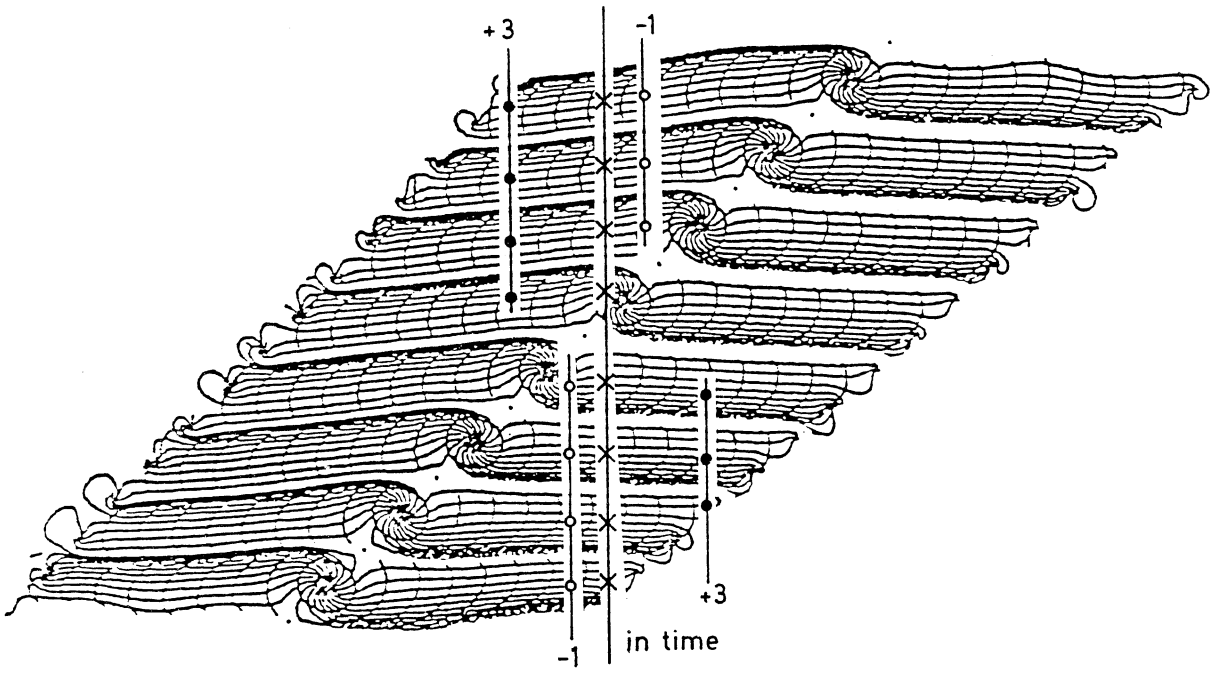

Fig. 2 Electron drift lines and isochrones. Superimposed on this is a high momentum track, together with its associated hits, and the apparent hits for a similar track from the previous bunch crossing or the one occuring three crossings later. Left-right ambiguities are omitted for clarity.

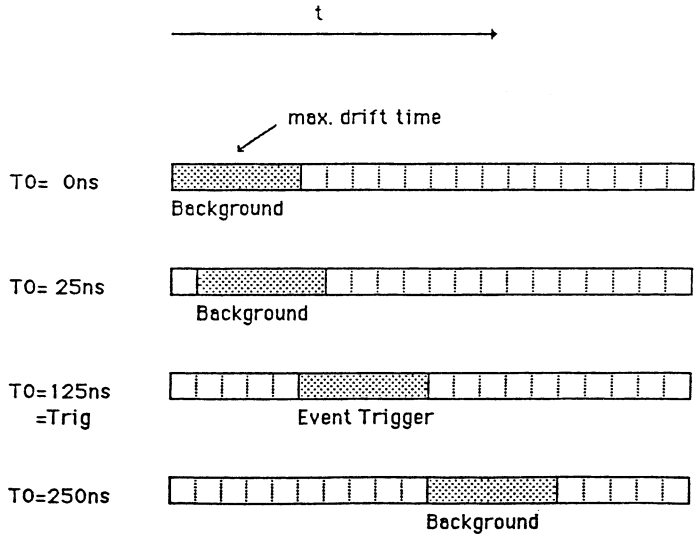

Fig. 3 The "Hit Buffer" associated with each wire at various bunch crossings T_o. The actual "Event Trigger" occurs at T_o = 125 ns whereas "Background Events" may occur at any of the earlier or later T_os. The shaded area corresponds to the range in which a valid hit can occur.

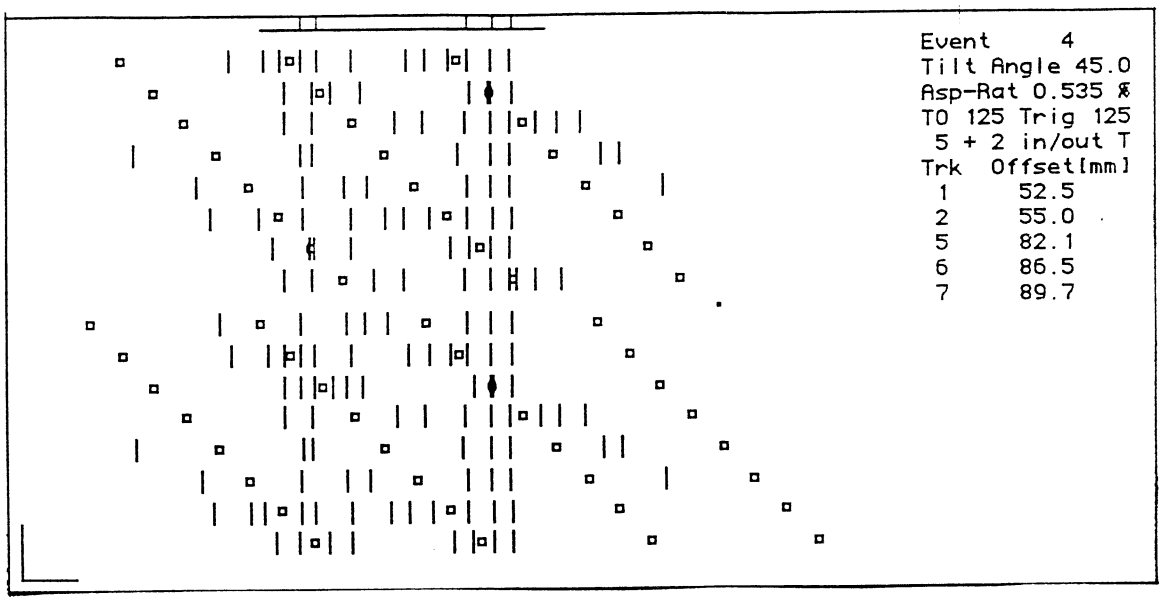

Fig. 4 A jet event with 5 tracks at the correct bunch crossing time T_o = 125 ns. Hits of each track are displayed together with the mirror hits. The positions of the generated tracks are indicated at the top. The line indicates the acceptance range, the tick marks above the line the positions of the generated tracks.

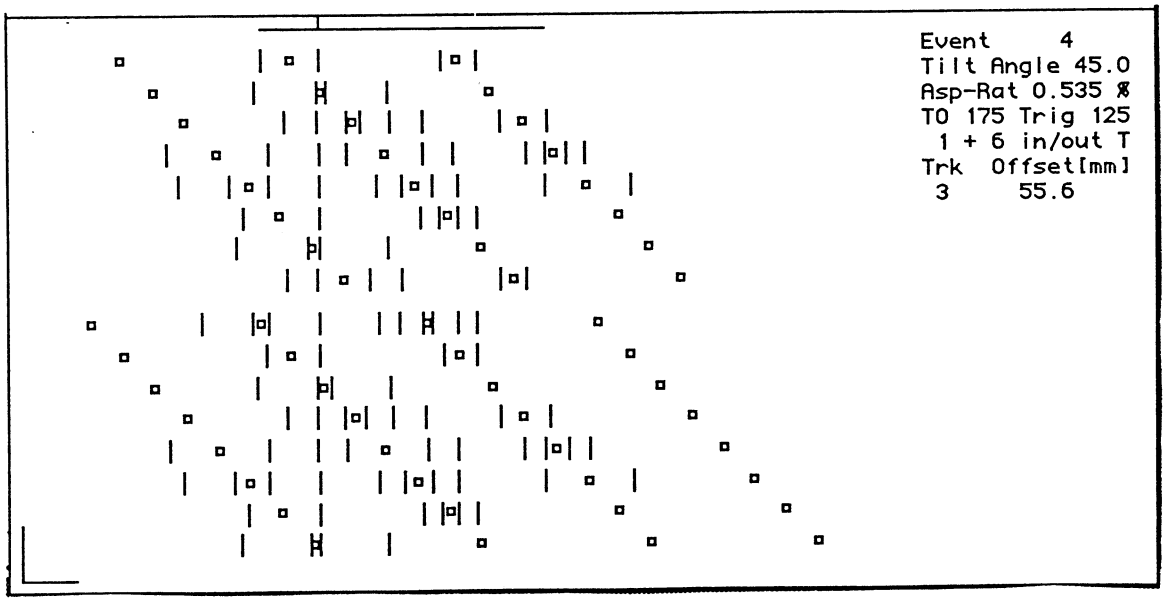

Fig. 5 The same raw data as in Fig. 4, but displayed assuming T_0 = 175 ns (i.e. two bunch crossings later). Due to the wire arrangement the jet tracks have completely dissolved into background hits whereas the track of a minimum bias event produced in the bunch crossing at T_0 = 175 ns is clearly recognized.

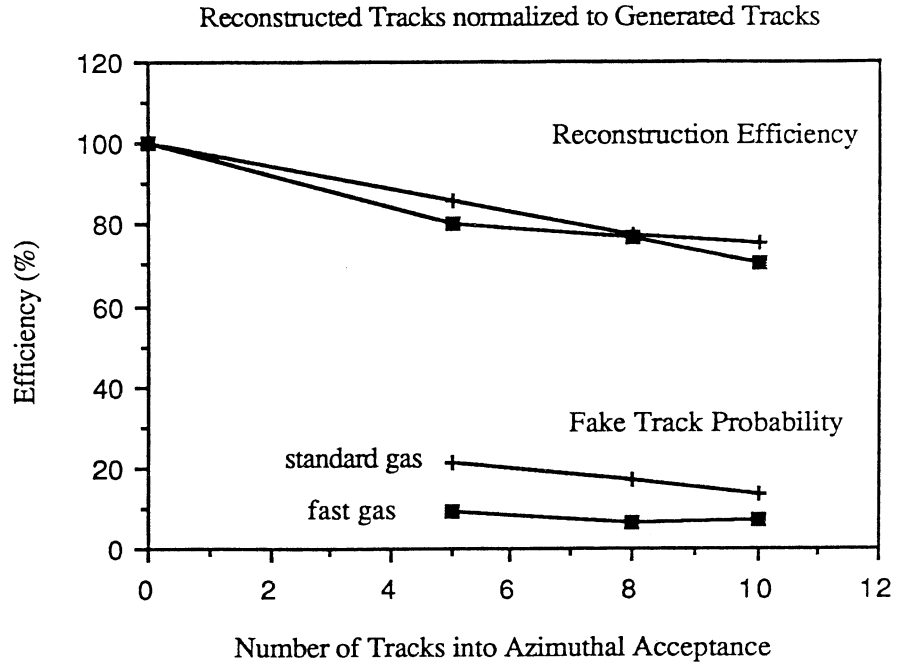

Fig. 6 The track reconstruction efficiency vs track density in a sector of 2° opening angle. The number of additional fake tracks normalized to the number of generated tracks is also indicated.

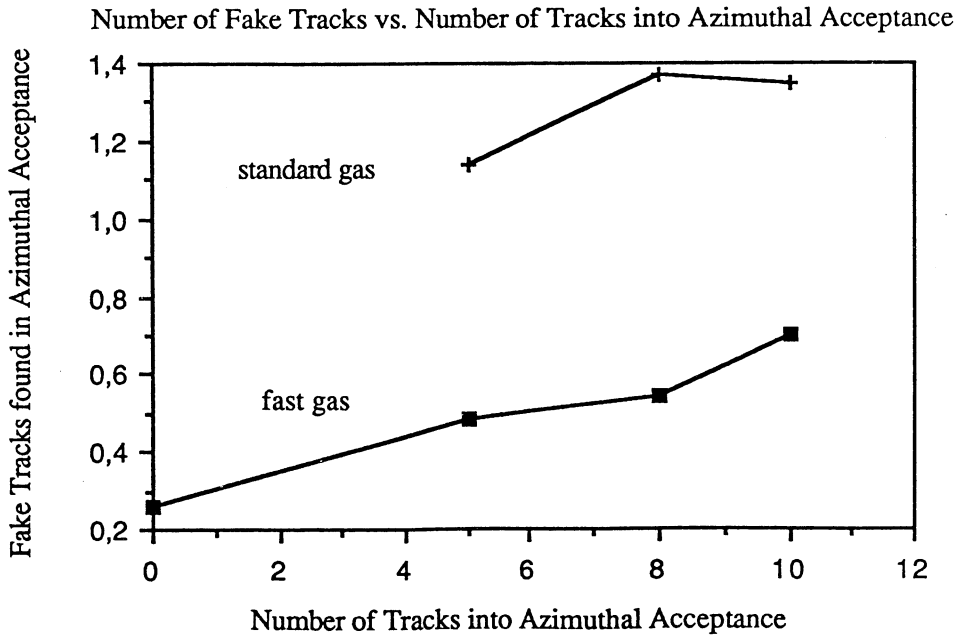

Fig. 7 The rate of fake tracks in a sector of 2° as a function of the track density.